Extraction and Analysis of T Waves in Electrocardiograms during Atrial Flutter

Vincent Jacquemet, Bruno Dubé, Réginald Nadeau, A. Robert LeBlanc, Marcio Sturmer, Giuliano Becker, Teresa Kus, Alain Vinet

Published in IEEE Trans. Biomed. Eng. (2011), vol. 58, no. 4, pp. 1104-1112

Abstract— **Analysis of T waves in the electrocardiogram (ECG) is an essential clinical tool for diagnosis, monitoring and follow-up of patients with heart dysfunction. During atrial flutter, this analysis has been so far limited by the perturbation of flutter waves superimposed over the T wave.**

This paper presents a method based on missing data interpolation for eliminating flutter waves from the ECG during atrial flutter. To cope with the correlation between atrial and ventricular electrical activations, the CLEAN deconvolution algorithm was applied to reconstruct the spectrum of the atrial component of the ECG from signal segments corresponding to TQ intervals. The location of these TQ intervals, where the atrial contribution is presumably dominant, were identified iteratively. The algorithm yields the extracted atrial and ventricular contributions to the ECG. Standard T-wave morphology parameters (T-wave amplitude, T peak – T end duration, QT interval) were measured.

This technique was validated using synthetic signals, compared to average beat subtraction in a patient with a pacemaker and tested on pseudo-orthogonal ECGs from patients in atrial flutter. Results demonstrated improvements in accuracy and robustness of T-wave analysis as compared to current clinical practice.

I. Introduction

The T wave of the surface lead electrocardiogram (ECG) reflects voltage gradients during ventricular repolarization [1]. Changes in T-wave morphology, amplitude and duration are considered to be significantly related to health, disease and sudden death. T-wave morphology is also modulated by heart rate, the autonomic nervous system and drugs affecting K^+ and Ca^{++} currents. The QT interval (from QRS onset to T-wave end) includes both ventricular depolarization and repolarization. Prolongation of this interval is used clinically to detect susceptibility to life threatening ventricular arrhythmias, notably torsades de pointes in the long QT syndromes [2], as well as a number of metabolic, electrolytic and drug-related effects. Abnormally short QT interval duration has also been related to arrhythmic risk [2].

Most studies have excluded the analysis of T-wave morphology and QT duration in atrial flutter mainly because of the superposition of atrial flutter waves on the T wave (Fig. 1A), resulting in a seemingly large variability in T-wave morphology (Fig. 1B). Indeed, in atrial flutter, the atria are activated by a stable macroreentrant depolarization wave at a rate of 230 to 350 bpm [3]. This electrical activity is manifested on the ECG as regular patterns of flutter waves (usually sawtooth-shaped, like in Fig. 1A). Untreated, the ventricles respond most frequently in a 2:1 ratio (≈150 bpm; every other beat being blocked by the atrio-ventricular node). When atrio-ventricular conduction is depressed (usually following medical intervention or pharmacological treatment), this ratio may be 3:1, 4:1 or higher, or it may be variable.

One approach to the treatment of atrial flutter is the administration of antiarrhythmic drugs prolonging (often non-uniformly) myocardial cellular action potentials. This is reflected on the ECG by an increase in QT interval duration [4]. Antiarrhythmic drugs such as sotalol, dofetilide and ibutilide may induce proarrhythmic effects [5]–[7]. These drug-induced arrhythmias are usually preceded by changes in T-wave morphology and QT interval prolongation. Careful monitoring of T waves is therefore an important target for ensuring the safety of antiarrhythmic drug administration.

Extraction of T waves requires separating the ventricular and the atrial contribution to the ECG. Signal processing techniques have been developed for that purpose, in particular for their application to atrial fibrillation. These techniques were based on spatiotemporal template subtraction [8]–[10], blind

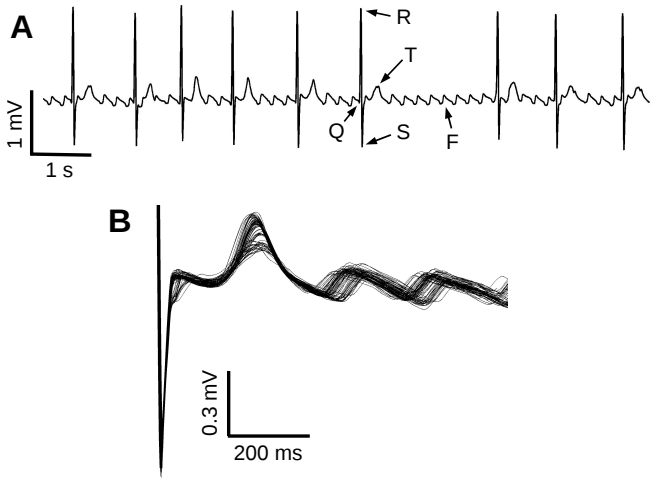

Fig. 1. (A) Example of ECG during atrial flutter (lead X of a pseudo-orthogonal lead system) along with the QRST nomenclature. The flutter wave is denoted by F. (B) 100 beats superimposed, aligned with the peak of their R wave.

This work was supported by the Natural Sciences and Engineering Research Council of Canada and by the Heart and Stroke Foundation of Québec.

All authors are with Centre de Recherche, Hôpital du Sacré-Coeur de Montréal, Montréal, Canada.

V. Jacquemet, A. R. LeBlanc and A. Vinet are also with Institut de Génie Biomédical & Département de Physiologie, Université de Montréal.

T. Kus is also with Département de Pharmacologie, Université de Montréal.

source separation [11], [12], and missing data interpolation in the QRS complex [9], [13]. In the case of atrial flutter, there is a clear causal relation between flutter waves and QRST complexes. The hypothesis of statistically independent atrial and ventricular components on which blind source separation is based is questionable. Moreover, phase shifts between QRS complexes and flutter waves are mainly due to variations in atrio-ventricular delay. Because the distribution of these phase shifts is most often limited to a narrow band (see Fig. 1B), methods based on the creation of QRST templates by averaging will not be sufficiently accurate. If QRST templates were used, only one QT interval value would be obtained for each template, thus forbidding beat-to-beat monitoring. Single beat methods relying on the dominant T wave (estimated as the principal component of the ST-T segment) for T-wave cancellation [9] require as many independent leads with similar T waves as possible. As a result, their applicability to pseudo-orthogonal 3-lead systems is limited. Missing data interpolation [13], however, is applicable to any type of atrial rhythm and any lead system provided that TQ intervals are long enough (*i.e.*, ventricular rate is not too fast) to enable data analysis.

This paper describes a method based on missing data interpolation for eliminating flutter waves from recordings of orthogonal lead ECG in case of atrial flutter with variable atrio-ventricular block. *A priori* knowledge about spectral properties of flutter waves is incorporated. A deconvolution technique is applied to account for possible integer ratios between atrial and ventricular rate. The ability of the method to estimate T wave parameters is validated using clinically-relevant synthetic signals and tested on 3-lead pseudo-orthogonal ECGs from patients in atrial flutter (type I).

II. Methods

A. Flutter Basic Frequency

The ECG signal $ECG(t)$ can be conceptually written as the sum of a ventricular component $V(t)$ and an atrial component $A(t)$. The baseline wandering is included in the ventricular component. An algorithm will be designed to estimate the atrial component by successive iterations $A_n(t)$. The T wave will be extracted from the signal $ECG(t)-A_n(t)$. The central hypothesis of our approach is that the atrial flutter $A(t)$ is a quasiperiodic signal (within a time window of 1 minute) with a power spectrum limited to frequency bands around a basic frequency f_0 and its harmonics. The algorithm processes each (pseudo-orthogonal) lead separately, although the VCG magnitude (RMS curve) is used for the detection of markers such as the offset of the T wave. Atrial activity is recovered by analyzing the ECG signal in the bands $[kf_0-\Delta f; kf_0+\Delta f]$ with $k=1,2,\ldots$ where Δf denotes the peak half-width. Peak width is associated with amplitude modulations (notably due to respiration whose frequency range typically lies within 0.1–0.3 Hz at rest) and possible frequency modulation (local changes in cycle length). Based on these empirical considerations as well as on direct measurement of peak width in clinical signals, Δf was set to 0.3 Hz. Estimation of the basic frequency f_0 is obtained by finding the maximal value in the power spectrum of $ECG(t)$ in the band 2.5–6 Hz. The absence of a clear peak at $f_0/2$ is checked. Because atrial signals may be small on some leads, f_0 is set to the median of the values obtained for all the leads. If necessary, advanced or multi-lead dominant frequency identification techniques can be used [13]–[17].

B. Spectrum of the Atrial Component

In the TQ interval, electrical activity in the ECG is dominated by the atrial contribution, while the ventricular component is a major factor in the QT interval. The atrial signal is considered as a time series with missing data in the QT interval [13]. Assuming that an estimate of the markers of the onset of the Q wave (Q_{on}) and the offset of the T wave (T_{off}) is available (see next Subsect.), the gap function $G(t)$ is defined as 0 in the intervals [Q_{on},T_{off}] and 1 otherwise. The function $G(t)$ is also set to zero during premature ventricular contractions, artifacts, saturation and pacemaker impulses (if any). The problem is now to recover the signal $A(t)$ when only the signal

$$A_{TQ}(t) = A(t)\cdot G(t) \tag{1}$$

can be observed. In the clinical application, $G(t)$ will be constructed based on estimated marker positions and $A_{TQ}(t)$ will be approximated by $ECG(t)\cdot G(t)$. In the Fourier domain (the hat $\hat{}$ denotes the Fourier transform), this relation becomes a convolution ($\star$):

$$\hat{A}_{TQ}(f) = \hat{A}(f) \star \hat{G}(f)\ . \tag{2}$$

The main signals involved in this method, as well as their power spectral density, are shown in Fig. 2. A major issue is that flutter waves periodically trigger a ventricular beat, and as a consequence the flutter basic frequency is often a multiple of the ventricular rate. The spectra of A and G therefore overlap. To perform this deconvolution, the CLEAN algorithm will be applied [18], [19]. This method iteratively uses an analytical formula valid for a single sine wave. Intuitively, each frequency component of $\hat{A}_{TQ}(f)$ is successively "moved" to the spectrum $\hat{A}(f)$ by exploiting the fact that $\hat{G}(f)$ is known. This approach was found to be particularly appropriate for signals with marked spectral components [18].

The CLEAN algorithm adapted for flutter signals can be outlined as follows:

1) Inputs: signals $A_{TQ}(t)$ and $G(t)$; basic frequency f_0 and peak half-width Δf
2) Compute the Fourier transforms $\hat{A}_{TQ}(f)$ and $\hat{G}(f)$; normalize $\hat{G}(f)$ so that $\hat{G}(0)=1$
3) Set the residual spectrum to $\hat{R}(f) := \hat{A}_{TQ}(f)$ and the estimated atrial spectrum to $\hat{A}(f) := 0$
4) Define the set $B(f_0) := \bigcup_{k\geq 1}[kf_0-\Delta f; kf_0+\Delta f]$
5) Iterate until $\max_f |\hat{R}(f)| < tol_c \cdot \max_f |\hat{A}_{TQ}(f)|$
   a) Find the frequency f_{peak} that maximizes $|\hat{R}(f)|$ in the frequency bands $B(f_0)$
   b) Compute the variable a (the star * denotes the complex conjugate):

$$a := \frac{\hat{R}(f_{\text{peak}}) - \hat{R}(f_{\text{peak}})^*\ \hat{G}(2f_{\text{peak}})}{1-|\hat{G}(2f_{\text{peak}})|^2} \tag{3}$$

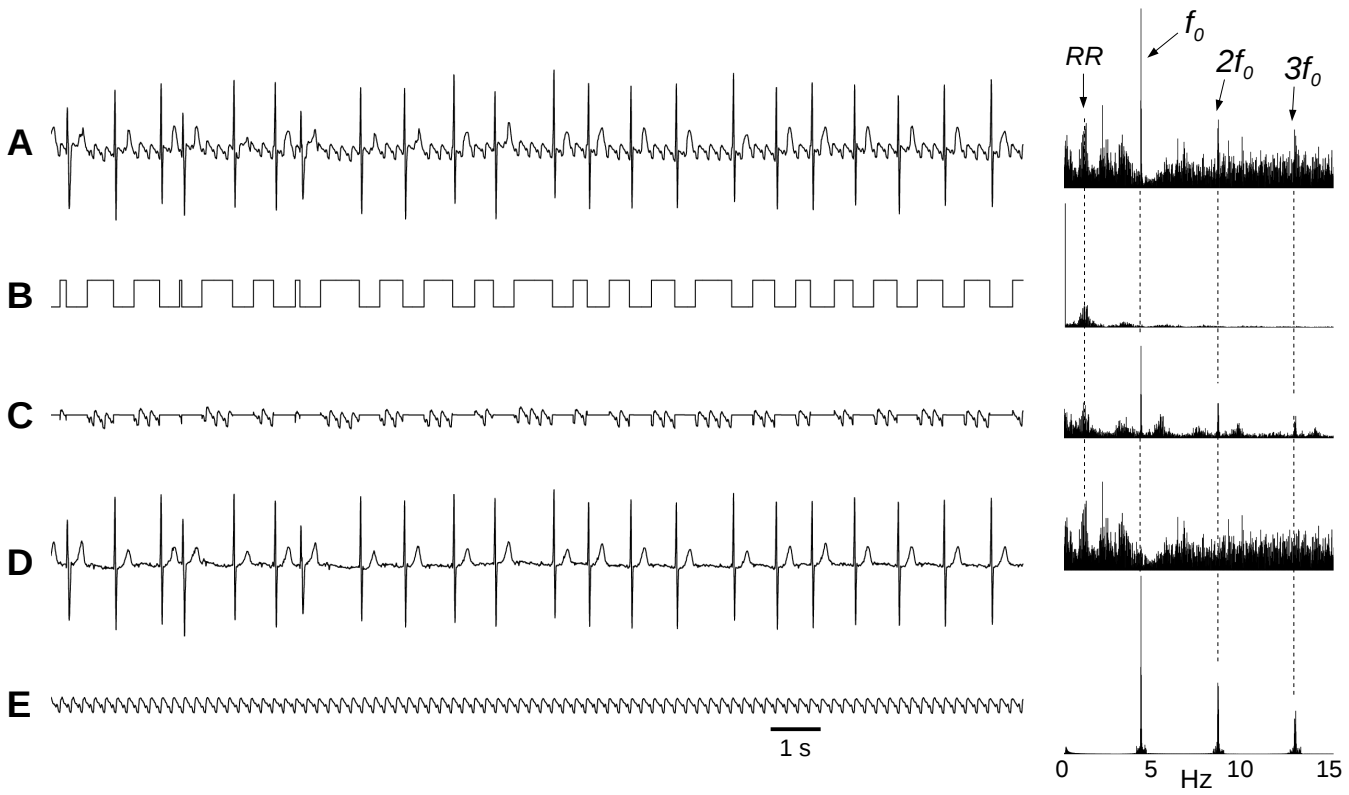

Fig. 2. Separation of atrial and ventricular components of the ECG in a patient with atrial flutter. *Left panels*: (A) ECG signal $ECG(t)$, lead X; (B) gap function $G(t)$; (C) the product of the two previous signals, denoted by $A_{TQ}(t)$; (D) resulting ventricular component $V(t)$; (E) resulting atrial component $A(t)$. *Right panels*: Corresponding power spectral densities; RR indicates average heart rate and f_0 is the flutter basic frequency.

c) Update the spectra (the gain g is a parameter such that $0 < g < 1$; $\delta(f)$ is the Dirac distribution):

$$\hat{R}(f) := \hat{R}(f) - g \cdot \Big(a\, \hat{G}(f - f_{\text{peak}}) + a^*\, \hat{G}(f + f_{\text{peak}}) \Big) \quad (4)$$

$$\hat{A}(f) := \hat{A}(f) + g \cdot \Big(a\, \delta(f - f_{\text{peak}}) + a^*\, \delta(f + f_{\text{peak}}) \Big) \quad (5)$$

6) Compute the inverse Fourier transform of $\hat{A}(f)$
7) Output: the atrial signal $A(t)$, extrapolated in the regions with missing data

Two parameters are involved in this deconvolution procedure: the gain g and the tolerance tol_c. In a way similar to underrelaxation, the gain accounts for possible interference (through the function $\hat{G}(f)$) between peaks and reduces the effect of the order the peaks are processed. The convention $\hat{G}(0) = 1$ simplifies Eq. (3) [19]. The tolerance tol_c is an estimate of the noise level. The values $g = 0.9$ and $tol_c = 0.5\%$ were selected empirically, guided by previous analyses of the CLEAN algorithm [18]–[20]. No significant difference was found after the parameter g was reduced from 0.9 to 0.5. Mathematical foundations of this algorithm, its convergence and its relation with least-square fit of sine functions were studied by Schwarz [21].

C. Iterative Identification of QT intervals

When QRST complexes are contaminated by atrial flutter waves, these is no clear isoelectric point. As a result, identification of the markers Q_{on} and T_{off} is not reliable. An iterative scheme was developed to isolate the QRST complexes from the atrial waves and improve Q_{on} and T_{off} detection. An initial estimate of the markers Q_{on} and T_{off} was used to define a gap function and extract an estimate of the atrial component in the ECG [22]. Then, the markers were updated using the ECG minus the estimated atrial component. Iterations were performed until QT intervals converged in the root-mean-square (RMS) sense. The algorithm is sketched below:

1) Inputs: $ECG(t)$
2) Initialization: set $V_0(t) := ECG(t)$ and $QT_0 = 0$; QT_n are vectors of size N where N is the number of processed QRST complexes
3) Iterate $n = 1, 2, \ldots$ until $\|QT_n - QT_{n-1}\| < tol_{qt} \cdot \sqrt{N}$
   a) Identify the markers Q_{on} and T_{off} in $V_{n-1}(t)$ and compute the sequence of QT intervals QT_n
   b) Form the gap function $G_n(t)$ from these markers and the location of artifacts identified in the original $ECG(t)$ signal by visual inspection
   c) Apply the CLEAN algorithm to the signal $ECG(t) \cdot G_n(t)$ with gap function $G_n(t)$ to get an estimate $A_n(t)$ of the atrial signal
   d) Set $V_n(t) := ECG(t) - A_n(t)$
4) Outputs: ventricular $V_n(t)$ and atrial $A_n(t)$ components

An ECG fiducial point detector [22] based on the magnitude of the VCG signal was applied to identify the markers Q_{on} and T_{off} in the signal $V_{n-1}(t)$. The marker T_{off} was defined as the intersection between the baseline and the tangent at the steepest negative slope of the T wave. The marker Q_{on} was defined as the position of the minimum of the Q wave when reporting QT intervals. To improve robustness and stability, a different definition of the marker Q_{on} was used to construct the gap function. A Gaussian was fitted to each R peak (VCG magnitude) based on peak position, height and width at half height. The marker Q_{on} was defined as the point of the fitted Gaussian preceding the peak at 0.1% of peak height. Before marker detection, baseline correction was reinforced. ECG signal range was limited to atrial wave amplitude by clipping larger deflections. The resulting signal was low-pass filtered at 1 Hz. This baseline curve was subtracted from the ECG only for marker detection. For all other purposes the standard 0.01–100 Hz preprocessing band-pass filter was sufficient. The tolerance for the exit criterion was set to $tol_{qt} = \Delta t$ where $\Delta t = 2$ ms is the sampling resolution.

D. Clinical and Synthetic Signals

Ten patients in stable type I atrial flutter scheduled to undergo catheter ablation were selected. Three-lead ECGs were continuously recorded at a sampling frequency of 500 Hz during the whole procedure (as well as 1 to 25 hours before and after) using standard Holter monitoring system (Burdick, Model 6632). Electrode configuration was designed to generate 3 pseudo-orthogonal leads X, Y and Z (X = V5 vs V6R; Y = S vs LL; Z = E vs V9). Sternal electrodes (E and S) come from the EASI lead system [23]; LL is the left leg electrode; V6R and V9 are extended precordial electrodes. All signals were band-pass filtered (0.01–100 Hz). In addition, ECGs were recorded in a patient with atrio-ventricular block and an implanted pacemaker whose configuration was set to fixed-rate pacing with a cycle length of 1500 ms for about 45 minutes.

To validate the signal processing methods, synthetic signals were generated by adding a ventricular and an atrial component derived from computer-manipulated clinical signals. The ventricular signals came from ECGs recorded with the same lead system, also at a sampling frequency of 500 Hz, in a patient in sinus rhythm during a tilt table test. As a result of the tilt test protocol, this ECG featured significant variations in heart rate and QT intervals. This enabled us to evaluate the ability of the algorithm to track changes in T-wave morphology. Segments of 80 s were extracted. Baseline correction was performed using cubic splines interpolated between silent points located before the onset of the P wave. P waves were removed and the cubic-spline baseline was reintroduced.

To simulate a flutter wave signal, a beat with a long RR interval and a stable atrial activity was selected in the ECG of a patient in atrial flutter. A period of the signal was extracted. This waveform was resampled (time scaling of the signal) and duplicated so that its basic frequency was a multiple of the ventricular rate (inverse of the median RR interval in the 80-s window). Atrial-to-ventricular rate ratios of 3:1 to 5:1 were simulated in order to span the typical range of atrial flutter (2.5 to 6 Hz). Atrial signals were scaled so that their amplitude was 0.5 to 1 times that of the T wave. Amplitude modulation was introduced to simulate the influence of respiration and other factors (sum of 5 sine waves with frequency 0.1, 0.15, 0.17, 0.2 and 0.21 Hz chosen empirically to mimick observed amplitude modulation, see [8], [13]; total amplitude of the modulation: 0 to 20% of atrial wave amplitude).

TABLE I

ROOT-MEAN-SQUARED ERROR (RMSE) ON THREE T-WAVE MORPHOLOGY PARAMETERS OBTAINED WITH THE SYNTHETIC SIGNALS FOR DIFFERENT ATRIAL TO VENTRICULAR (A:V) RATE RATIOS (MEAN±SD AND MEAN RELATIVE RMSE; $N = 160$)

A:V	QT RMSE (ms)	TpTe RMSE (ms)	VMTmax RMSE (μV)
Flutter wave amplitude = 1 × T-wave amplitude			
3:1	6.3±2.6 (1.7%)	5.4±2.0 (6.3%)	17.9±5.6 (5.1%)
3.5:1	5.2±2.4 (1.4%)	4.7±2.1 (5.5%)	23.0±8.0 (6.6%)
4:1	5.1±2.0 (1.4%)	4.5±2.2 (5.3%)	28.6±9.6 (8.1%)
4.5:1	3.9±2.0 (1.1%)	4.2±2.0 (5.0%)	19.3±4.5 (5.5%)
5:1	4.4±1.9 (1.2%)	4.1±1.7 (4.8%)	17.6±5.0 (5.0%)
Flutter wave amplitude = 0.5 × T-wave amplitude			
3:1	5.0±2.3 (1.4%)	4.5±1.9 (5.3%)	10.1±4.0 (2.9%)
3.5:1	4.0±2.3 (1.1%)	3.8±2.0 (4.5%)	14.2±5.2 (4.0%)
4:1	4.3±1.9 (1.2%)	3.8±2.1 (4.5%)	20.0±6.4 (5.7%)
4.5:1	3.4±2.0 (0.9%)	3.6±2.0 (4.2%)	13.5±3.7 (3.8%)
5:1	4.1±2.0 (1.1%)	3.5±1.7 (4.1%)	12.0±4.4 (3.4%)

E. Data Analysis

Both synthetic and clinical ECGs were analyzed by segments of 80 s in which stationarity of atrial activity was assumed. This gave a frequency resolution of 0.0125 Hz in the Fourier domain. The first and last 10 s of each segment were discarded to avoid boundary effects. Implementation of the signal processing techniques was streamlined to enable direct import and export of ECG data in the native format of the ECG analysis software Burdick Vision Premier Holter (Cardiac Science, Bothell, WA, USA). After suppression of atrial activity, QRST complexes were analyzed. T-wave morphology was described by the following parameters: QT interval (QT), interval from the peak of the T wave to the end of the T wave (TpTe), and maximal amplitude of the T wave on the VCG magnitude (VMTmax). To reduce the dependency in heart rate, corrected QT interval (QTc) was computed using the standard Bazett's formula $\mathrm{QTc} = \mathrm{QT}/\sqrt{\mathrm{RR}}$, where RR (in seconds) is the RR interval averaged over the previous 60 beats. Beat-to-beat variations were quantified by computing the RMS value of the difference between consecutive beats; for example, $\Delta\mathrm{TpTe}_n = \mathrm{TpTe}_n - \mathrm{TpTe}_{n-1}$ and RMS $\Delta\mathrm{TpTe} = \left((N-1)^{-1}\sum_{n=2}^{N}\Delta\mathrm{TpTe}_n^2\right)^{1/2}$ where N is the number of beats recorded. Data were reported as mean±standard deviation (SD) computed over all the segments.

III. RESULTS

A. Validation with Synthetic Signals

Synthetic signals were generated with 3:1, 3.5:1, 4:1, 4.5:1 and 5:1 atrial to ventricular rates, a flutter wave amplitude of 0.5 and 1 times that of the T-wave, and amplitude modulations

of 0%, 5%, 10%, 15% and 20%. Each of these 50 signals were split into 32 segments of length 80-s associated with different ventricular rates and QT intervals. Ventricular rate ranged from 55 to 78 bpm (66±8 bpm) and QT ranged 320 to 410 ms (364±23 ms). The flutter wave subtraction algorithm was applied to all 1600 signals. Convergence was reached after 2 to 4 iterations, 3 iterations in 88% of the cases. QRST morphology parameters QT, TpTe and VMTmax were measured on these processed signals. Original signals (without atrial component) served as reference to define root-mean-squared error (RMSE). RMSE are reported in Table I as a function of the ratio of atrial to ventricular rate. No significant differences in RMSE were found when the amplitude of the flutter wave was time-dependent (0 to 20% amplitude modulation with frequencies < 0.3 Hz). Since sampling resolution was $\Delta t = 2$ ms, RMSE on QT and TpTe were of the order of 2 to 4 Δt. RMSE on marker position was therefore typically of the order of 1 to 2 Δt for synthetic signals. Reduction in atrial wave amplitude as compared to the T wave resulted in lower errors.

B. Comparison with Average Beat Subtraction

There is a case to which average beat subtraction is applicable: when a patient in atrial flutter with atrio-ventricular block also has a pacemaker stimulating the ventricles at a fixed rate. In this patient, the phase of flutter waves is not correlated with the timing of R waves. R-wave aligned beat averaging therefore eliminates (stationary quasi-periodic) flutter waves. Moreover, QRST complexes are expected to be very stable because of the fixed rate. We took advantage of this situation to compare our T-wave extraction method to standard average beat subtraction [8].

A sequence of 3000 consecutive beats were extracted from a 3-lead Holter ECG (at rest) of a patient in flutter with a pacemaker stimulating at a cycle length of 1500 ms. Flutter basic frequency was 3.18 Hz. Ectopic/abnormal/non-paced beats were rejected based on RR time series. The R waves of the remaining 2204 beats were aligned and averaged for each of the 3 leads. The phase shift between flutter waves (in the TQ interval) of different aligned beats was computed using the largest positive peak of the cross-correlation function. The resulting distribution of phase shifts was not statistically different from a uniform distribution between 0 and the period of flutter (p=0.28; Kolmogorov-Smirnov test). This suggests that the average beat should be free of atrial component provided the flutter wave is stable enough.

Figure 3 compares the average beat computed without flutter wave cancellation (thick black line) to a set of 800 R-wave aligned beats after flutter wave cancellation (thin gray lines). T-wave extracted by the two methods were consistent. Although the flutter wave cancellation algorithm does not remove noise and baseline wander, it enables the analysis of beat-to-beat variations in T-wave morphology. Note that U wave (which lies within the TQ interval) was not eliminated because only a narrow frequency band was considered around flutter basic frequency and its harmonics. QT interval was stable at 514±5 ms (range 498–525 ms), as expected during fixed rate pacing and in agreement with the result obtained using the average beat method (see Fig. 3). In contrast, QT interval measured with the same method directly on raw signals contaminated with flutter waves (the approach currently used in clinical practice) was more scattered, with values ranging from 492 to 565 ms (527±13 ms).

C. T-Wave Morphology in Patients with Atrial Flutter

When ventricular electrical activity was driven by atrial flutter, no reference T wave was available for comparison. To demonstrate how flutter wave cancellation can improve T-wave analysis and diagnosis, statistics of T-wave morphology parameters were computed and compared to those obtained in the absence of flutter wave cancellation (current clinical practice). T waves were extracted and analyzed in 10 patients at rest with atrial flutter before catheter ablation (2 to 25 hours Holter recording). For all patients, in the vast majority of the 80-s segments, 3–4 iterations were sufficient to reach convergence. An example of ventricular component extraction is displayed in Fig. 2. Two cases with regular rhythm (stable 4:1 and 3:1 atrioventricular block during several minutes) are shown in Fig. 4. Although the atrial spectrum was partially masked by the harmonics of the ventricular activity, accurate F-wave cancellation was achieved by the deconvolution method. Amplitude distribution of reconstructed atrial waves was approximately Gaussian-shaped. The coefficient of variation (SD/mean) of atrial wave amplitudes ranged from 5.5% to 32% (average: 13.5%), which is comparable to the values used for synthetic signals.

Table II presents statistics for corrected QT intervals measured on patient ECGs before and after flutter wave cancellation, and during sinus rhythm (after catheter ablation, when available) since QTc is used by clinicians to identify abnormal conditions. Patients are ordered according to their ratio between T-wave amplitude and flutter wave amplitude measured on the VCG magnitude signal. In raw ECG signals, T waves appear prolonged or shortened due to the superposition of flutter waves (Fig. 2A). Increased robustness to this perturbation is achieved by measuring QT interval

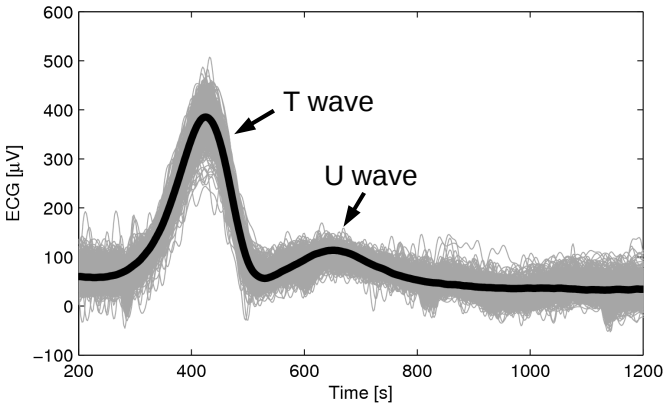

Fig. 3. T waves extracted from the ECG (lead X) recorded during flutter in a patient with a pacemaker (fixed pacing rate). The R peak is located at $t = 50$ ms (not shown). *Thick black line*: average beat computed without flutter wave cancellation; *Thin gray lines*: 800 R-wave aligned beats after flutter wave cancellation.

TABLE II

CORRECTED QT INTERVALS (QTC) IN PATIENTS MEASURED ON RAW ECG SIGNALS DURING FLUTTER, ECGS AFTER FLUTTER WAVE CANCELLATION, AND ECGS DURING SINUS RHYTHM.

			QTc (raw data)		QTc (after cancellation)		QTc (sinus rhythm)	
patient	# beats	T/F	mean±SD [ms]	range [ms]	mean±SD [ms]	range [ms]	mean±SD [ms]	range [ms]
1	67805	5.8	421 ± 21	[397, 463]	409 ± 14	[388, 435]	399 ± 9	[385, 415]
2	85780	4.4	437 ± 20	[410, 471]	431 ± 16	[409, 460]	N/A	
3	3157	3.8	450 ± 11	[419, 465]	432 ± 15	[413, 455]	438 ± 15	[416, 453]
4	102128	3.5	391 ± 30	[357, 442]	373 ± 23	[345, 412]	369 ± 14	[352, 397]
5	10405	2.4	454 ± 18	[435, 491]	448 ± 11	[434, 463]	429 ± 14	[411, 451]
6	17223	2.3	386 ± 18	[362, 422]	372 ± 10	[359, 389]	N/A	
7	15071	2.3	414 ± 31	[378, 475]	409 ± 19	[380, 444]	N/A	
8	7541	1.9	463 ± 34	[401, 508]	392 ± 22	[360, 426]	N/A	
9	6886	1.8	414 ± 30	[379, 477]	401 ± 12	[386, 423]	391 ± 7	[381, 401]
10	8204	0.8	422 ± 22	[385, 453]	447 ± 23	[413, 489]	440 ± 13	[425, 461]

beats: number of beats analyzed; T/F: ratio between the amplitude of T wave and that of the flutter wave; SD: standard deviation; range: interval from the 5th to the 95th percentile; N/A: not available.

TABLE III

RMS VALUE OF BEAT-TO-BEAT VARIATIONS MEASURED IN RAW SIGNALS AND AFTER FLUTTER WAVE CANCELLATION

			RMS ΔQTc [ms]			RMS ΔTpTe [ms]			RMS ΔVMTmax [μV]		
patient	# beats	T/F	raw	corrected	ratio	raw	corrected	ratio	raw	corrected	ratio
1	67805	5.8	16.6	13.9	0.84	5.1	4.4	0.86	144.0	105.7	0.73
2	85780	4.4	18.0	13.9	0.77	15.3	4.8	0.32	81.3	57.7	0.71
3	3157	3.8	16.2	20.4	1.26	16.2	6.2	0.38	163.8	43.8	0.27
4	102128	3.5	21.5	14.9	0.69	16.7	10.3	0.62	46.8	46.5	0.99
5	10405	2.4	21.9	12.4	0.57	21.7	11.0	0.51	55.9	46.6	0.83
6	17223	2.3	20.3	9.6	0.48	14.3	8.0	0.56	97.1	32.0	0.33
7	15071	2.3	39.8	20.1	0.51	35.7	16.8	0.47	78.1	56.4	0.72
8	7541	1.9	44.3	30.9	0.70	35.5	12.6	0.36	180.0	132.7	0.74
9	6886	1.8	39.8	11.3	0.28	27.5	7.2	0.26	101.6	44.0	0.43
10	8204	0.8	17.6	30.0	1.70	19.1	19.9	1.04	109.7	62.5	0.57

beats: number of beats analyzed; raw: measured before flutter wave cancellation; corrected: measured after flutter wave cancellation; T/F: ratio between the amplitude of T wave and that of the flutter wave;

duration on the VCG. Measures of QTc statistical dispersion are generally reduced by flutter wave cancellation to values closer to those obtained during sinus rhythm. In particular, the 95th percentile of QTc is often decreased by about 30 ms. An exception is patient 10. Because T-wave amplitude is smaller than flutter waves, the fiducial point detector is confused unless flutter waves are suppressed (values are consistently smaller by 25 ms). The values of QTc intervals before and after ablation (flutter vs sinus rhythm) are in agreement with each other. This provides an evidence of the validity of the method for clinical data, although repolarization (and consequently, QTc) is not expected to necessarily stay the same after ablation due to possible changes in physiological conditions (autonomic nervous system, inflammation).

The interference caused by flutter waves is expected to affect beat-to-beat variations in T-wave morphology parameters when measured directly in raw signals. To quantify this effect, the RMS value of beat-to-beat differences in each parameter was computed before and after flutter wave cancellation. Table III shows that the flutter wave cancellation algorithm significantly reduced beat-to-beat variations in QTc, TpTe and VMTmax. Beat-to-beat fluctuations in QTc measured in raw signals were smaller when T-wave amplitude was larger as compared to flutter wave amplitude (Table III, 4th column). The remaining variations may be associated with rapid changes in heart rhythm (due to a different degree of atrio-ventricular block). Two exceptions were observed in patient data. Patient 3 had a pacemaker; larger beat-to-beat variations in QT intervals were caused by inaccurate identification of Q_{on} due to pacemaker impulse artifacts (TpTe and VMTmax were not affected though). Patient 10 had very small T-wave amplitude on all leads; in the absence of flutter wave cancellation, the end of a flutter wave was consistently (and incorrectly) identified as T_{off}, so measured QTc beat-to-beat variations were smaller than expected.

IV. DISCUSSION

An algorithm for the suppression of atrial flutter waves in the ECG was designed and validated. In contrast with QRST cancellation techniques developed for atrial fibrillation signals, our approach concentrates on the quality of the extracted ventricular component rather than on the elimination of artifacts in the extracted atrial signal. It also enables the integration of *a priori* spectral information about the atrial component. By design, the content in the atrial component was kept to the minimum: noise, baseline variations, artifacts were considered as part of the ventricular component and processed at a later stage. A crucial point for the success of flutter wave cancellation was to avoid overfitting the data in the TQ interval. Significant baseline drift within the beat, a U-wave or small artifacts could lead to incorrect interpolation of missing atrial data in the QRST complex. Figure 3 shows the ability of the proposed method to retain ventricular contributions (such as the U wave) within the TQ interval. The parameter

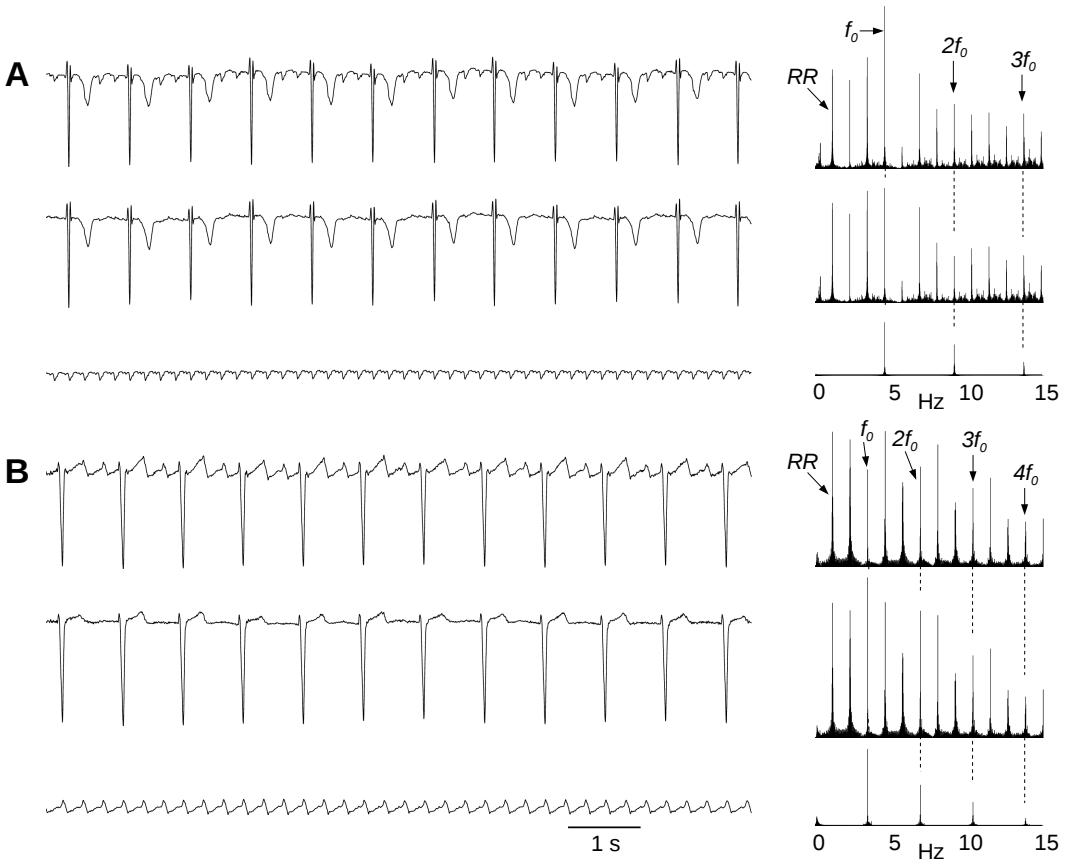

Fig. 4. Examples of ventricular activity extraction in patients with regular heart rhythm during flutter. *Upper signal*: original ECG; *middle signal*: ECG after flutter-wave cancellation; *lower signal*: flutter waves; corresponding spectra are shown on the right; RR indicates average heart rate and f_0 is the flutter basic frequency. (A) 4:1 atrioventricular block, lead Y; (B) 3:1 atrioventricular block, lead Z. In case (B), some peak amplitudes are larger in the ventricular component than in the original signal because the atrial and the ventricular components are negatively correlated.

Δf constraining the spectral content of the atrial component controls the trade-off between an accurate reproduction of the TQ interval and a reasonable and robust interpolation in the QT interval. Two other parameters are involved in the CLEAN algorithm. The signal-to-noise ratio parameter (tol_c) ensures that the background noise is not included in the atrial signal. The gain factor (g) makes it possible to handle interferences between spectral peaks through the Fourier transform of the gap function. In our application, results were found to be insensitive to g in the range 0.5 to 0.9.

Fiducial point detection is an important element of the algorithm. An initial estimate of Q_{on} and T_{off} has to be computed based on the ECG contaminated by flutter waves. The use of VCG magnitude for marker identification addresses the problem of small amplitude T waves on some leads. To ensure convergence of the iterative QT interval identification process, marker localization needs to be robust to noise. Baseline correction was also found to be critical. This is why Q_{on} was defined based on the R peak height and width (instead of the minimum preceding the R wave) when constructing the gap function G. Once atrial wave suppression is performed, any measure of QT interval can be used.

A limitation shared with many QRST cancellation techniques is the necessity to have sufficient information in the TQ intervals over a segment (1 minute), which may not be the case when heart rate is very high (for instance, most cases of stable 2:1 atrioventricular block). Note, however, that our approach still applies if premature contraction, ventricular arrhythmia or transient 2:1 atrioventricular block (see 3rd beat in Fig. 2) occur for a limited time or if the RR time series shows an alternation of short (almost no TQ interval) and long intervals. When signal-to-noise ratio is low (small T-wave amplitude, like patient 10 in Table II and III, accuracy is reduced but no analysis would be reliable in this case in the absence of flutter wave cancellation. If a stable 2:1 block is present for more than one minute, in each ventricular beat the first F wave is masked by the QRS complex and the second is hidden in the T wave. A priori knowledge about atrial or ventricular activity or spatial information from many leads might be needed to perform their separation. In the absence of such information, T wave parameters may be extracted directly from the lead with smallest F wave amplitude.

Another limitation is the assumption that atrial cycle length and flutter wave morphology are relatively stable within each one-minute segment. Our approach is able to track both slow variations (time scale of several minutes) and respiratory modulations in atrial cycle length (time scale of 3 to 10 ventricular beats; see II-A). However, ventricular contraction

may modulate the morphology of the atrial contribution to the ECG [24] by moving or constraining atrial geometry and by affecting blood pressure. Ravelli et al. demonstrated that this effect can cause fluctuations in atrial cycle length within a ventricular beat [25], [26]. It remains a major challenge to account for this effect hidden in the T wave. In the worst case, this local time shift creates a short-duration artifact proportional to the time derivative of the F wave. Although these artifacts may affect the separation of atrial and ventricular activity, they have a limited impact on QT interval measurement.

The flutter wave cancellation algorithm opens the way for the analysis of QT–RR relationship during atrial flutter, extending similar analysis performed in sinus rhythm [27]. The relevance of this application is supported by QTc values extracted during flutter being consistent with those measured during sinus rhythm (Table II) and by the reduction in beat-to-beat variations after flutter wave cancellation (Table III). The performance of the algorithm on synthetic signals (Table I) and the comparison with average beat subtraction (Fig. 3) indicate that other parameters describing T-wave morphology could be investigated as well.

V. Conclusion

We developed and validated a new method for flutter wave cancellation in the ECG in order to facilitate the analysis of T wave during atrial flutter. This method assumes that flutter wave cycle length and morphology is stable over one-minute windows and that ventricular rate is not too high to enable data extraction from TQ intervals. This will provide clinicians with a convenient tool to monitor, diagnose and investigate the dynamics of ventricular repolarization in patients with atrial flutter.

References

[1] C. Antzelevich, "Cellular basis for the repolarization waves of the ECG," in *Dynamic Electrocardiography*, M. Malik and A. J. Camm, Eds. Blackwell-Futura, NY, 2004, pp. 291–300.

[2] H. Morita, J. Wu, and D. P. Zipes, "The QT syndromes: long and short," *Lancet*, vol. 372, no. 9640, pp. 750–63, 2008.

[3] A. L. Waldo, "Atrial flutter: From mechanism to treatment," in *Clinical approaches to tachyarrhythmias*, A. J. Camm, Ed. Futura Publishing, Armonk, NY, 2001, pp. 1–56.

[4] Y. G. Yap and A. J. Camm, "Drug-induced long QT syndrome," in *Clinical approaches to tachyarrhythmias*, A. J. Camm, Ed., vol. 16. Futura Publishing, Armonk, NY, 2002, pp. 2–16.

[5] D. Darbar, "Standard antiarrhythmic drugs," in *Cardiac Electrophysiology: From Cell to Bedside*, D. P. Zipes and J. Jalife, Eds. Saunders-Elsevier, Philadelphia, PA, 2009, pp. 959–973.

[6] C. Torp-Pedersen, M. Moller, P. E. Bloch-Thomsen, L. Kober, E. Sandoe, K. Egstrup, E. Agner, J. Carlsen, J. Videbaek, B. Marchant, and A. J. Camm, "Dofetilide in patients with congestive heart failure and left ventricular dysfunction. Danish investigations of arrhythmia and mortality on dofetilide study group," *N Engl J Med*, vol. 341, no. 12, pp. 857–65, 1999.

[7] B. S. Stambler, M. A. Wood, K. A. Ellenbogen, K. T. Perry, L. K. Wakefield, and J. T. VanderLugt, "Efficacy and safety of repeated intravenous doses of ibutilide for rapid conversion of atrial flutter or fibrillation. ibutilide repeat dose study investigators," *Circulation*, vol. 94, no. 7, pp. 1613–21, 1996.

[8] M. Stridh and L. Sornmo, "Spatiotemporal QRST cancellation techniques for analysis of atrial fibrillation," *IEEE Trans Biomed Eng*, vol. 48, no. 1, pp. 105–11, 2001.

[9] M. Lemay, J.-M. Vesin, A. van Oosterom, V. Jacquemet, and L. Kappenberger, "Cancellation of ventricular activity in the ECG: evaluation of novel and existing methods," *IEEE Trans Biomed Eng*, vol. 54, no. 3, pp. 542–6, 2007.

[10] P. Langley, J. J. Rieta, M. Stridh, J. Millet, L. Sornmo, and A. Murray, "Comparison of atrial signal extraction algorithms in 12-lead ECGs with atrial fibrillation," *IEEE Trans Biomed Eng*, vol. 53, no. 2, pp. 343–6, 2006.

[11] J. J. Rieta, F. Castells, C. Sanchez, V. Zarzoso, and J. Millet, "Atrial activity extraction for atrial fibrillation analysis using blind source separation," *IEEE Trans Biomed Eng*, vol. 51, no. 7, pp. 1176–86, 2004.

[12] F. Castells, J. J. Rieta, J. Millet, and V. Zarzoso, "Spatiotemporal blind source separation approach to atrial activity estimation in atrial tachyarrhythmias," *IEEE Trans Biomed Eng*, vol. 52, no. 2, pp. 258–67, 2005.

[13] R. Sassi, V. D. A. Corino, and L. T. Mainardi, "Analysis of surface atrial signals: time series with missing data?" *Ann Biomed Eng*, vol. 37, no. 10, pp. 2082–92, 2009.

[14] S. Pehrson, M. Holm, C. Meurling, M. Ingemansson, B. Smideberg, L. Sornmo, and S. B. Olsson, "Non-invasive assessment of magnitude and dispersion of atrial cycle length during chronic atrial fibrillation in man," *Eur Heart J*, vol. 19, no. 12, pp. 1836–44, 1998.

[15] F. Sandberg, M. Stridh, and L. Sornmo, "Frequency tracking of atrial fibrillation using hidden Markov models," *IEEE Trans Biomed Eng*, vol. 55, no. 2 Pt 1, pp. 502–11, 2008.

[16] Y. Prudat and J.-M. Vesin, "Multi-signal extension of adaptive frequency tracking algorithms," *Signal Processing*, vol. 89, no. 6, pp. 963–973, 2009.

[17] M. Lemay, Y. Prudat, V. Jacquemet, and J.-M. Vesin, "Phase-rectified signal averaging used to estimate the dominant frequencies in ECG signals during atrial fibrillation," *IEEE Trans Biomed Eng*, vol. 55, no. 11, pp. 2538–47, 2008.

[18] D. Roberts, J. Lehar, and J. Dreher, "Time series analysis with Clean-Part one- Derivation of a spectrum," *The astronomical journal*, vol. 93, p. 968, 1987.

[19] S. Baisch and G. Bokelmann, "Spectral analysis with incomplete time series: an example from seismology," *Computers and Geosciences*, vol. 25, no. 7, pp. 739–750, 1999.

[20] V. Vityazev, "Time series analysis of unequally spaced data: Intercomparison between estimators of the power spectrum," in *Astronomical Data Analysis Software and Systems VI*, vol. 125, 1997, p. 166.

[21] U. Schwarz, "Mathematical-statistical description of the iterative beam removing technique (method CLEAN)," *Astron. Astrophys*, vol. 65, no. 2, pp. 345–356, 1978.

[22] B. Dube, A. LeBlanc, J. L. Dutoy, D. Derome, and R. Cardinal, "PC-based ST-segment monitoring with the VCG," in *Proc. Engineering in Medicine and Biology Conference*, vol. 4, 1988, pp. 1768–1770.

[23] G. E. Dower, A. Yakush, S. B. Nazzal, R. V. Jutzy, and C. E. Ruiz, "Deriving the 12-lead electrocardiogram from four (EASI) electrodes," *J Electrocardiol*, vol. 21 Suppl, pp. S182–7, 1988.

[24] V. Jacquemet, B. Dubé, P. van Dam, A. R. LeBlanc, R. Nadeau, M. Sturmer, T. Kus, and A. Vinet, "Modulation of ECG atrial flutter wave amplitude by heart motion: A model-based and a bedside estimate," *Comput. Cardiol.*, vol. 37, 2010 (in press).

[25] F. Ravelli, M. Mase, and M. Disertori, "Mechanical modulation of atrial flutter cycle length," *Prog Biophys Mol Biol*, vol. 97, no. 2-3, pp. 417–34, 2008.

[26] M. Mase, L. Glass, and F. Ravelli, "A model for mechano-electrical feedback effects on atrial flutter interval variability," *Bull Math Biol*, vol. 70, no. 5, pp. 1326–47, 2008.

[27] E. Pueyo, P. Smetana, P. Caminal, A. B. de Luna, M. Malik, and P. Laguna, "Characterization of QT interval adaptation to RR interval changes and its use as a risk-stratifier of arrhythmic mortality in amiodarone-treated survivors of acute myocardial infarction," *IEEE Trans Biomed Eng*, vol. 51, no. 9, pp. 1511–20, 2004.

Vincent Jacquemet received the M.Sc. degree in physics in 2000 from the Swiss Federal Institute of Technology, Lausanne (EPFL), Switzerland, and the Ph.D. degree in biomedical engineering in 2004 from the Signal Processing Institute of EPFL. The topic of his thesis was the development of biophysical models of atrial fibrillation. Then he worked as a postdoc researcher in the Lausanne Heart Group at EPFL. Between 2007 and 2009, he was with the Department of Biomedical Engineering at Duke University with a "fellowship for advanced researcher" awarded by the Swiss National Science Foundation. Since 2009, he is researcher at Université de Montréal and Hôpital du Sacré-Coeur de Montréal. His research interests include complex dynamical systems, biophysical modeling, numerical simulation and signal processing.

Bruno Dubé received a B.Sc. degree in physics and biophysics and a M.Sc.A. degree in biomedical engineering, both from the Université de Montréal, Montreal, QC, Canada, in 1980 and 1984, respectively. Since 1984, he has been a Research Engineer and Computer Analyst at Sacré-Coeur Hospital, Montreal. His research interests include modeling of cardiac electrophysiological phenomena and digital signal processing.

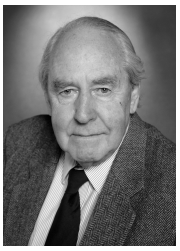

Réginald Nadeau received his M.D. degree from Université de Montréal in 1957 and his diploma in cardiology in 1964. In 2005, he became Emeritus Professor of Medicine and Physiology, Faculty of Medicine, Université de Montréal. In 1972, he founded the Research Center of Hôpital du Sacré-Coeur de Montréal and was Director from 1972 to 1997. He has practiced cardiology, in particular electrophysiology, since 1972 and has been involved in basic and clinical research.

A. Robert LeBlanc is Professor Emeritus of Biomedical Engineering at the Université de Montréal since 2009. He graduated in electrical engineering in 1967 and received a M.Sc. in 1970 and a D.Sc.A. in 1974, both in biomedical engineering and all from Ecole Polytechnique de Montréal. He has been head of the Biomedical Engineering Institute for over 10 years, a joint Institute between the Université de Montréal, Faculty of Medicine and the Ecole Polytechnique de Montréal. He is associate director of Research, Development and Valorization of the Research Center of Hôpital du Sacré-Coeur de Montréal since 1999. His research program is in the cardiovascular domain. It involves signal processing and mathematical modeling in both ischemic process and cardiovascular control.

Marcio Sturmer received his medical degree at the UFRGS in Brazil, 1994. He became a cardiologist at the Heart Institute in Porto Alegre, Brazil. From 2000 to 2004, he had his training in Cardiac Electrophysiology at the Heart Institute (Montreal University) in Montreal, Canada, and a training in Atrial Fibrillation ablation at the San Raphaele Hospital, in Milan, Italy. Since 2004 he has been Cardiac Electrophysiologist at the Sacré-Coeur Hospital of Montreal and University of Montreal. He is presently the Chief of the Electrophysiology Laboratory of the Sacr e-Coeur Hospital in Montreal.

Giuliano Becker graduated from the medical school at Santa Maria Federal University, Brazil in 1998. He received the diploma in internal medicine in 2000 and in cardiology in 2002. Between 2005 and 2008 he had his fellowship in cardiac arrhythmias and electrophysiology at Sacré-Coeur Hospital, Montreal (Canada) and he finished his fellowship with a complementary year in Rouen, France. Since 2009 he has been working at Sacré-Coeur Hospital as a cardiologist-electrophysiologist.

Teresa Kus received the Ph.D. degree in Pharmacology in 1978 and the M.D. degree in 1979 from McGill University, Montreal, Canada. She was trained in Internal Medicine, Cardiology with a subspecialty in cardiac electrophysiology and is currently director of the arrhythmia service at Hôpital du Sacré-Coeur in Montreal and Associate Professor in the Department of Pharmacology at the Université de Montréal. Her research interests include antiarrhythmic drugs, the role of the autonomic nervous system in vasovagal syncope and atrial arrhythmias.

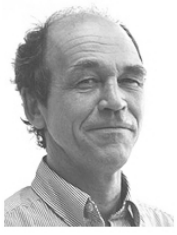

Alain Vinet received a B.Sc. and then a M.Sc. degree in physics from University of Montréal, Canada, in 1978. After working as a statistician and research assistant, he returned for a Ph.D. in Biomedical Engineering at the Institute of Biomedical Engineering, U. of Montréal, which he completed in 1989. After a two years post-doc in the pharmacology department of the Suny Health Science Center in Syracuse, N.Y., he became a researcher and then a professor at the Institute of Biomedical Engineering, U. of Montréal, where he is currently full professor since 2006. His research interests include modeling, nonlinear dynamics and computer simulation of cardiac tissue, bioelectric signal analysis and clinical statistics.